UCSF
UC San Francisco Previously Published Works

Title

NF2 Loss Promotes Oncogenic RAS-Induced Thyroid Cancers via YAP-Dependent Transactivation of RAS Proteins and Sensitizes Them to MEK Inhibition.

Permalink

https://escholarship.org/uc/item/12n09067

Journal

Cancer Discovery, 5(11)

Authors

Garcia-Rendueles, Maria
Ricarte-Filho, Julio
Untch, Brian
et al.

Publication Date

2015-11-01

DOI

10.1158/2159-8290.CD-15-0330

Peer reviewed

eScholarship.org Powered by the California Digital Library
University of California

Author Manuscript

Author Manuscript

Author Manuscript

Author Manuscript

HHS Public Access

Author manuscript

Cancer Discov. Author manuscript; available in PMC 2016 May 01.

Published in final edited form as:

Cancer Discov. 2015 November ; 5(11): 1178–1193. doi:10.1158/2159-8290.CD-15-0330.

NF2 loss promotes oncogenic RAS-induced thyroid cancers via YAP-dependent transactivation of RAS proteins and sensitizes them to MEK inhibition

Maria E.R. Garcia-Rendueles[1,#], **Julio C. Ricarte-Filho**[1,#], **Brian R. Untch**[1,2], **Iñigo Landa**[1], **Jeffrey A. Knauf**[1,6], **Francesca Voza**[1], **Vicki E. Smith**[1], **Ian Ganly**[2], **Barry S. Taylor**[1,3], **Yogindra Persaud**[1], **Gisele Oler**[1], **Yuqiang Fang**[4], **Suresh C. Jhanwar**[4], **Agnes Viale**[5], **Adriana Heguy**[1], **Kety H. Huberman**[5], **Filippo Giancotti**[7], **Ronald Ghossein**[4], and **James A. Fagin**[1,6,7]

[1]Human Oncology and Pathogenesis Program, Memorial Sloan Kettering Cancer Center, New York, NY, 10065

[2]Department of Surgery, Memorial Sloan Kettering Cancer Center, New York, NY, 10065

[3]Department of Epidemiology and Biostatistics, Memorial Sloan Kettering Cancer Center, New York, NY, 10065

[4]Department of Pathology, Memorial Sloan Kettering Cancer Center, New York, NY, 10065

[5]Marie-Josée and Henry R. Kravis Center for Molecular Oncology, Memorial Sloan Kettering Cancer Center, New York, NY, 10065

[6]Department of Medicine and [7]Cell Biology Program, Memorial Sloan Kettering Cancer Center, New York, NY, 10065

[7]Department of Medicine, Weill Cornell Medical College, New York, NY, 10065, USA

Abstract

Ch22q LOH is preferentially associated with *RAS* mutations in papillary and in poorly differentiated thyroid cancer (PDTC). The 22q tumor suppressor *NF2*, encoding merlin, is implicated in this interaction because of its frequent loss of function in human thyroid cancer cell lines. *Nf2* deletion or *Hras* mutation are insufficient for transformation, whereas their combined disruption leads to murine PDTC with increased MAPK signaling. Merlin loss induces RAS signaling in part through inactivation of Hippo, which activates a YAP-TEAD transcriptional program. We find that the three *RAS* genes are themselves YAP-TEAD1 transcriptional targets, providing a novel mechanism of promotion of RAS-induced tumorigenesis. Moreover, pharmacological disruption of YAP-TEAD with verteporfin blocks RAS transcription and signaling, and inhibits cell growth. The increased MAPK output generated by NF2 loss in *RAS*-

Correspondence: James A. Fagin, MD, Department of Medicine and Human Oncology and Pathogenesis Program, Memorial Sloan-Kettering Cancer Center, 1275 York Avenue, Box 296, New York, NY 10065, faginj@mskcc.org, Phone: 646-888-2136.
[#]Equal contributors.

The authors disclose no potential conflicts of interest.

Author Manuscript Author Manuscript Author Manuscript Author Manuscript

mutant cancers may inform therapeutic strategies, as it generates greater dependency on the MAPK pathway for viability.

Introduction

Neurofibromatosis type 2 is an autosomal dominant syndrome caused by germline heterozygous mutations of *NF2*, which encodes Merlin. It is characterized by tumors of the nervous system such as schwannomas, meningiomas and ependymomas. The associated neoplasias often harbor loss of heterozygosity (LOH) of the chromosome 22q region encompassing the *NF2* gene (1). Other malignancies associated with *NF2* defects include mesotheliomas, melanomas and clear cell renal cancers.

Merlin inhibits cell growth in response to cell contact. It interacts with multiple partners to modulate distinct pathways including Hippo (2), receptor tyrosine kinases (RTK) (3, 4), Rac/Cdc42/p21-activated kinases (PAK) (5–7) and mTOR (8, 9). Merlin also has a nuclear function by inhibiting the $CRL4^{DCAF1}$ E3 ubiquitin ligase (10). Hippo is an evolutionarily conserved kinase cascade that suppresses tissue overgrowth through phosphorylation of YAP, leading to its sequestration in the cytoplasm and disrupting its ability to promote transcriptional enhancer activation domain (TEAD)-dependent transcription of genes involved in proliferation and survival (11–14). Despite the critical role of the Hippo pathway in growth control, *NF2* is the only commonly mutated cancer gene in this pathway(15). The lineage-specific properties and the genetic repertoire intrinsic to different cancer types may predispose NF2-deficient cells to be preferentially addicted to distinct pathways. For instance, Merlin loss activates effectors of mTOR in meningiomas, schwannomas and mesotheliomas and confers sensitivity to rapamycin (8, 9, 16). In glial cells, merlin loss induces cell growth in an Erbb2-dependent manner (17). By contrast, hepatocellular carcinomas in mice with hepatocyte-targeted deletion of *Nf2* have been variously reported to be dependent on Hippo (18) or on EGFR signaling (19).

Papillary thyroid cancers (PTC) are indolent tumors associated with mutually exclusive mutations of *BRAF*, *RAS* and of fusion RTK oncogenes, such as *RET*, *NTRK1* and *NTRK3* (20). The driver frequency is different in poorly differentiated (PDTC) and anaplastic thyroid cancers (ATC), in that the latter are enriched for *RAS* mutations (21–23). Here we show that *NF2* is a novel thyroid tumor suppressor, preferentially associated with *RAS* mutations. Although loss of *Nf2* or *Ras* activation is insufficient to independently induce thyroid cancers in mice, their combination is highly tumorigenic. *NF2* loss cooperates with mutant *RAS* to increase signaling via MAPK, acting in part through YAP-induced transcriptional activation of oncogenic and wild-type RAS, providing a novel mechanism of promotion of RAS-induced tumorigenesis. This has therapeutic implications, as these and other inputs resulting from merlin deficiency converge to confer preferential sensitivity to selective MEK inhibitors *in vitro* and in mouse genetic models of the disease. In addition, pharmacological disruption of the YAP-TEAD transcriptional complex decreases expression of oncogenic and wild-type RAS and inhibits tumor cell growth.

Author Manuscript Author Manuscript Author Manuscript Author Manuscript

Results

Loss of chromosome 22q in PTC, advanced thyroid cancers and thyroid cancer cell lines

The Cancer Genome Atlas recently completed an analysis of ~ 400 PTCs, which showed a high frequency of ch22q loss in *RAS*-mutant PTC (45% had 22q LOH) (24) (Supplementary Table S1). The association was particularly striking for *HRAS*: 10/14 (71%) ($p<5 \times E-6$; OR >10). ch22q is the only region of copy number variation in the genomes of most of these cancers, which are otherwise diploid, suggesting that one or more tumor suppressors on 22q play an important role in tumorigenesis. We found that PDTCs also had a high frequency of 22q LOH (14/63; 22%) as determined by SNP-CGH and/or copy number analysis of sequence reads derived from an exon capture NGS panel of 341 cancer genes, 6 of which mapped to Ch22q (Supplementary Table S1; Supplementary Fig. S1A–D). Although most tumors had LOH of all 6 genes, spanning the majority of the chromosome arm, *CHEK2*, *NF2* and *EP300* were consistently lost. As was the case in PTC, Ch22q LOH in PDTCs was seen preferentially in association with *RAS* (8/16; 50%) as compared to *BRAF*-mutant tumors (0/26). Five of the 20 ATCs were *RAS* mutant, one of which had 22q LOH (Supplementary Table S1).

Of the cancer genes mapping to Ch22q, we focused in greater detail on *NF2* because 3/40 thyroid cancer cell lines had homozygous nonsense mutations of this gene (Cal62: c. 643G>T, pE215*; 8505c: c.385G>T, p.E129* and TCO-1: c.303T>A, p.Y101*). In addition, the KHM-5M ATC cell line had a homozygous deletion of exon 4 of *NF2* that disrupts the central FERM domain of merlin, previously reported in neurofibromatosis patients (25) (Supplementary Fig. S2). Consistent with the low frequency of homozygous NF2 inactivation in cell lines, there are limited data supporting biallelic NF2 inactivation in primary thyroid cancers. Indeed, *NF2* mutations in tumor samples were rare other than for one ATC with a somatic G>A substitution at the −1 position of the intron 14/exon 15 boundary (splice donor site), which removes exon 15 and impairs the biological effects of merlin (26). As ATCs are heavily infiltrated with macrophages, which decrease sensitivity of genomic profiling, we expanded the analysis of *NF2* copy number by performing FISH on ATC tissue microarrays, which showed that 10/16 had NF2 LOH, one of which had a homozygous deletion (Supplementary Fig. S3A,B).

Several thyroid cancer cell lines that were wild-type or hemizygous for *NF2* had very low or absent merlin mRNA and/or protein levels (Supplementary Fig. S4A, B). Despite lower NF2 mRNA, we did not detect aberrant methylation patterns of CpG islands in the promoter of *NF2* in cell lines or tumors (not shown). Interestingly, the Hth74 ATC cell line had a markedly decreased NF2 mRNA half-life (Supplementary Fig. S4C). Hence, as reported in other lineages, loss of merlin in thyroid cancers occurs through diverse mechanisms (Supplementary Fig. S4D): LOH or intragenic deletions, somatic base substitutions as well as posttranscriptional events (27–30).

Mice with thyroid-specific activation of *Hras^{G12V}* and *Nf2* loss develop PDTC

In view of the strong association between *NF2* and *RAS* in human thyroid cancers, we next explored the potential biological significance of this interaction in mouse models.

Author Manuscript Author Manuscript Author Manuscript Author Manuscript

Endogenous expression of *Hras*^{G12V} in thyroid cells was achieved by activating the latent *FR-Hras*^{G12V} allele by crosses with *TPO-Cre* mice (31) (Fig. 1A). None of the *TPO-Cre*/*FR-Hras*^{G12V} heterozygous or homozygous animals developed thyroid cancer. Although ~ 65% of mice with thyrocyte-specific homozygous deletion of *Nf2* (*TPO-Cre/Nf2*^{flox2}) exhibited mild nodular hyperplasia after 18 months, none developed cancer (Supplementary Table S2). By contrast, *TPO-Cre/FR-Hras*^{G12V}/*Nf2*^{flox2} mice developed large thyroid cancers with high penetrance (Fig. 1B). Most of these were PDTCs, and were associated with a marked increase in pERK (Fig. 1C).

Enforced merlin expression inhibits growth of human NF2-null thyroid cancer cells and attenuates RAS-induced signaling

We next investigated mechanisms accounting for the NF2-RAS interactions seen *in vivo* in *RAS*-mutant human thyroid cancer cell lines. Re-expression of wild-type (WT) merlin in *RAS*-mutant / *NF2*-null Cal62 and Hth83 cells decreased growth and colony formation in soft agar, whereas the loss-of-function mutant NF2-L64P (32) was without effect (Fig. 2A). NF2, but not NF2-L64P also decreased pMEK and pERK in these cells (Fig.2B). Conversely, knockdown of merlin in *HRAS*-mutant /*NF2*-WT C643 cells enhanced growth and MAPK signaling (Fig. 2C).

Merlin loss enables sequestration of Rich1, a GTPase activating protein, by a tight junction protein complex, which de-represses Rac1, leading to activation of Raf-MEK signaling (33). We found that this pathway was also operative in the setting of constitutively activated RAS (Supplementary Fig. S5). Expression of merlin suppressed Rac1-GTP as well as phosphorylation of its effector p21-activated kinase (PAK) at S141 and T423. This in turn decreased CRAF and MEK phosphorylation at S298, a PAK substrate. In a reciprocal experiment, merlin silencing was associated with increased pPAK-T423 (Supplementary Fig. S5A, B).

Expression of a dominant negative PAK construct (PAK1 83–149) modestly suppressed growth of KRAS^{G12R}/NF2 null Cal62 cells. As predicted, this was associated with decreased phosphorylation of the PAK substrate S298-MEK. However, pS217/p221-MEK and pERK were not significantly reduced, suggesting that, in the context of mutant RAS, merlin loss augments MAPK signaling through alternative mechanisms (Supplementary Fig. S5C). Consistent with this, the effects of merlin on PAK signaling were apparent 24h after dox-induction (Supplementary Fig. S5B), whereas pS217/p221-MEK and pERK were seen to decrease beginning at 48h (Fig. 2B). The ATP-competitive PAK kinase inhibitor FRAX597 also preferentially suppressed PAK phosphorylation in merlin-silenced C643 cells, with no apparent effects on pERK (Supplementary Fig. S5D). It also inhibited cell growth after merlin knockdown, although it was toxic at higher concentrations, possibly through off-target effects.

Upon cell-cell contact merlin reportedly prevents internalization and signaling of the epidermal growth factor receptor (EGFR) by sequestering it into an insoluble membrane compartment (3, 4). The impairment of EGFR signaling by merlin also manifests in *RAS*-mutant thyroid cancer cell lines. Although merlin loss augments EGFR signaling, this does not appear to contribute significantly to growth regulation (Supplementary Fig. S6).

Author Manuscript Author Manuscript Author Manuscript Author Manuscript

NF2 loss leads to increased expression of mutant and wild-type RAS through YAP-dependent transcriptional activation

To explore the possible contribution of other inputs upstream of RAS to MAPK activation, we measured RAS-GTP levels prior to and 72h after merlin expression. Unexpectedly, merlin inhibited both WT and mutant RAS-GTP, which was associated with decreased protein and mRNA levels of all RAS isoforms (Fig. 3A, B). Conversely, knockdown of NF2 increased mutant and wild type RAS mRNA and protein levels in NF2-WT cells (Fig. 3C). Strikingly, this was also the case in the mouse models of the disease. Thus, protein levels of the three *Ras* genes were markedly increased in thyroid tissues with conditional deletion of *Nf2*. This was associated with increased pERK and pMEK in *TPO-Cre/Hras*^{G12V}*/Nf2*^{flox2} mice, presumably because of overexpression of the oncogenic *Hras* allele (Fig. 3D). Copy number abnormalities of *Hras* were found in a subset of these tumors (Supplementary Fig. S7). However, this does not account for the consistent increase in Hras in all tumors we examined, or the higher expression of the wild-type Ras proteins.

Consistent with the known interaction of merlin with the Hippo pathway, expression of WT-merlin in NF2-null RAS-mutant cell lines resulted in YAP phosphorylation and retention in the cytoplasm, with reciprocal changes seen after knockdown of merlin in NF2 wild-type cells (Fig. 4A, B). YAP is a required component of a transcriptional regulatory complex that includes its close homologue TAZ, and TEAD. Silencing of YAP in Cal62 (KRAS^{G12R}, NF2 null) cells decreased mRNA levels of all RAS isoforms, as well as of the canonical YAP-transcriptional target CTGF (Fig. 4C). This was associated with a profound decrease of all three RAS proteins (Fig. 4D). YAP knockdown also prevented the induction of RAS protein and of MAPK signaling by merlin silencing in C643 (HRAS^{G13R}, NF2-WT) cells (Fig. 4E) and inhibited growth of NF2-null cell lines (Fig. 4F). Consistent with this, expression of constitutively active YAP1^{S127A} in C643 cells (NF2-WT) induced RAS gene expression (Fig 4G) and promoted cell growth (Fig. 4H). YAP1^{S127A} also rescued the growth inhibition (Fig 4I) and the suppression of RAS mRNA levels by merlin in Cal62 cells (Fig. 4J). In silico analysis identified consensus TEAD binding sites in the promoters of the three *RAS* genes (Fig. 5A). The functional relevance of this prediction is supported by ChIP-PCR with antibodies to either YAP or TEAD1 (TEAD1 is the most abundant TEAD isoform in thyroid cancer cells – see Supplementary Fig. S8A). This showed that merlin expression markedly diminished occupancy by YAP and TEAD1 of TEAD consensus motifs in the promoters of the three RAS genes (Fig. 5B and Supplementary Fig S8B).

Verteporfin (VP) is an FDA-approved drug used as a photosensitizer for photodynamic ablation of abnormal blood vessels in patients with macular degeneration (34). VP was identified in a drug screen for compounds that could disrupt YAP-TEAD driven transcription, and shown to inhibit YAP-dependent growth (14). We found that VP inhibited growth of NF2-null Cal62 (Fig. 5C) and Hth83 cells (Supplementary Fig. S8C), an effect that was dampened by merlin expression (Supplementary Fig S8D). VP decreased YAP and TEAD, lowered Ras protein abundance and inhibited MAPK signaling. Reciprocal findings were seen in C643 cells after merlin silencing (Supplementary Fig. S8E). VP treatment inhibited TEAD occupancy of the oncogenic *KRAS* gene promoter in Cal62 cells (Fig. 5D).

Author Manuscript Author Manuscript Author Manuscript Author Manuscript

Hence, genetic and pharmacological disruption of YAP-TEAD leads to decreased oncogenic RAS gene expression, MAPK signaling and growth.

NF2/Merlin deficiency sensitizes RAS-mutant cancer cells and murine PDTC to MEK inhibition

We next explored whether the increased MAPK signaling seen in RAS mutant/NF2-deficient thyroid cancer cell lines rendered them more dependent on this pathway for growth. This was explored in isogenic lines derived from C643 cells ($HRAS^{G13R}$, NF2-WT) modified to stably express sh-NF2 (Fig. 6A). Although expression of oncogenic HRAS, as well as baseline pMEK and pERK, were markedly higher in the merlin-depleted shNF2-M4 line, the inhibition of the pathway by the MEK inhibitor was comparable. Despite this, growth suppression by AZD6244 was greater in cells depleted of merlin. We also tested a set of 7 RAS-mutant thyroid cancer cell lines for growth response to MEK inhibition. There was a trend for greater sensitivity to AZD6244 in RAS mutant thyroid cancer cell lines that were merlin null or low as compared to merlin wild-type cell lines (Supplementary Fig. S9A). To explore the contribution of distinct inputs into MEK (i.e. Rac1-PAK vs canonical Ras-RAF), we explored growth in response to AZD6244, FRAX597 or their combination in C643 cells with or without merlin silencing. Consistent with the data shown in Fig. 6, C643-shNF2.M2 cells are exquisitely sensitive to the MEK inhibitor. Although knockdown of merlin also sensitizes cells to growth inhibition by the PAK inhibitor, the effects were comparatively modest. Combined inhibition showed only modest additive effects (Supplementary Fig. S9B).

We also examined the effects of AZD6244 in three models of $Hras^{G12V}$-driven mouse poorly differentiated thyroid cancers, arising in the context of *Nf2*, *Pten* or *p53* homozygous loss. All of these gave rise to PDTCs, defined based on the presence of necrosis and a high mitotic rate on histology. These tumors differed, however, in tumor doubling time (Pten=Nf2>>p53) (Supplementary Fig S10A), and overall survival (Supplementary Fig S10B). *Hras/Nf2* and *Hras/p53* tumors stained intensely for pERK, whereas *Hras/Pten* tumors had low pERK and increased pAKT staining (Fig 6B). Treatment of mice with *$Hras^{G12V}$/Nf2-null* thyroid cancers with AZD6244 resulted in a greater and more consistent reduction of tumor size than in cancers arising in *Has^{G12V}/Pten-null* or *$Hras^{G12V}$/p53-null* mice (Fig. 6C). IHC of treated tumors showed marked reduction of pERK staining in all three tumor types, whereas pAKT IHC remained very high in *Hras/Pten* tumors, possibly accounting for their lack of response to therapy (Fig. 6D).

Discussion

The striking tissue overgrowth phenotypes induced by genetically disabling the core components of the Hippo pathway in *Drosophila melanogaster* prompted exploration of its role in mammalian cell proliferation and cancer development (13). Hippo inactivation converges to regulate gene expression through the transcriptional coactivator YAP and/or its close homolog TAZ. This raises the question of how the YAP/TEAD transcriptional targets may impact the biology of cancers driven by oncogenes, such as RAS, which nominally operate through a distinct canonical signaling network. Our finding that RAS genes are

Author Manuscript Author Manuscript Author Manuscript Author Manuscript

themselves transcriptionally regulated by YAP may have profound implications for RAS-driven tumors.

The importance of *Ras* mutant allele gene dosage for transformation is well established. A requirement for intensification of mutant Ras signaling through copy-number imbalances is supported by studies in *Hras* mutant fibroblasts, in which transformation is strongly associated with amplification of the mutant allele (35). Increased mutant allele copy number is an obligate early event in $Hras^{G12V}$-induced papilloma development (31, 36, 37). Similarly, the aggressiveness of myeloproliferative neoplasms expressing $Nras^{G12D}$ is augmented when the mutant allele is homozygous (38). Moreover, the expression of oncogenic RAS in human cancer cell lines is consistently higher than that of the other wild type RAS proteins (38). Although *HRAS* gene amplification has been reported in thyroid cancer (39), the overall frequency, at least in PTC, appears to be low (24). Despite the critical significance of mutant Ras protein abundance on its signaling and transforming properties, there is so far limited information on how other oncogenic inputs may alter its expression. The 3'UTRs of human *RAS* genes contain multiple complementary sites to the let-7 family of microRNAs, which regulate RAS expression by translational inhibition and/or by decreasing mRNA stability (40, 41). Loss of let-7 miRs increases Ras protein levels, and conversely let-7 overexpression decreases them and attenuates oncogenic Ras-induced tumorigenesis (41, 42).

Regulation of mutant *RAS* gene transcription as a functional consequence of disrupting a parallel oncogenic pathway has, to our knowledge, not been previously implicated as a mechanism of tumor promotion. The YAP-TEAD complex modulates expression of a diverse array of transcriptional targets (12). However, comparatively little is known about the specific YAP-regulated genes responsible for mediating the effects of Hippo inactivation on growth, invasiveness, metastases or senescence (43–46). CTGF is a prototypical target of YAP-TEAD, and has been functionally implicated in hepatocellular growth and tumorigenesis (47). YAP1 was recently reported to rescue viability of pancreatic cancer cells conditionally expressing mutant Kras after oncoprotein withdrawal in mice. The authors implicated genes co-regulated by YAP1 and E2F in this process, many of which were cell cycle regulators (48). In a screen for genes promoting survival of *KRAS*-mutant cells following oncogene silencing *in vitro*, YAP1 was the most prominent hit among those that could also activate either MAPK or PI3K signaling. YAP1 was found to regulate a set of immediate response genes that were also activated by KRAS, ultimately converging on the transcription factor FOS, which also rescued cells after KRAS silencing (49). YAP is also required for $Kras^{G12D}$-induced pancreatic transformation in mice, by inducing expression of genes encoding secreted factors that promote cancer cell growth and the establishment of a tumorigenic stromal microenvironment (50). We do not yet know whether YAP1-mediated transcriptional activation of RAS mRNAs is ubiquitous or context dependent, or if this may have contributed to some of the observations in the lineages and models described above. Our analysis of previously published genome-wide Chip-Seq data in mouse embryonic stem cells points to clear YAP-binding peaks in all three *RAS* genes ((51); not shown), suggesting that these are likely to be regulated via Hippo inactivation in other cell types as well. However, tissue overgrowth induced by Hippo silencing likely requires the concerted

Author Manuscript Author Manuscript Author Manuscript Author Manuscript

regulation of genes involved at multiple key steps of the process. As RAS proteins are critical signaling nodes, modulation of their expression would impact the signal amplitude emanating from a wide array of upstream inputs.

The studies described above implicate YAP as an important effector in RAS-mutant cancer. However, the mechanisms causing YAP activation in these contexts is not known. In the case of *RAS*-mutant thyroid cancer, merlin loss-of-function is a key event (Fig. 7A,B). Although germline or somatic *NF2* mutations are primarily implicated in the pathogenesis of nervous system tumors, mesotheliomas, melanomas and renal cell carcinomas, mice with heterozygous *Nf2* mutation develop a broader range of tumors, which lose the wild-type allele (52). Loss-of function of merlin also occurs in the absence of homozygous deletion or mutation, through aberrant splicing, mRNA loss, calpain-mediated proteolysis, proteasomal degradation, or phosphorylation (27–30, 53). Consistent with this, several thyroid cancer cell lines that were merlin-null or low did not have homozygous genomic *NF2* mutations. This is particularly relevant in advanced thyroid cancer, as intragenic NF2 mutations are rare in tumors with 22q LOH. The extent by which NF2 haploinsufficiency is associated with impaired expression of the wild type allele in human tumors is currently uncertain. Hence, sensitive protein-based assays may need to be developed to screen cancers for merlin loss of function, particularly if this proves to be an actionable event.

There are potential therapeutic opportunities resulting from Hippo pathway inactivation in the context of RAS-induced tumorigenesis. We found that these tumors hyperactivate MAPK signaling, and consequently generate increased dependency on this pathway for viability. Thus, although merlin loss leads to a global increase in YAP-TEAD transcriptional output, the genes that augment susceptibility to MEK inhibition are paramount in this setting. Moreover, as illustrated by our data with VP, targeting of YAP may prove to be viable strategy for thyroid, and perhaps other cancers, driven by oncogenic RAS.

Experimental Procedures

Sample collection and DNA isolation

A total of 83 advanced thyroid tumors, including 20 anaplastic (ATC) and 63 poorly differentiated thyroid cancers (PDTC) were assessed. Both frozen (n=37) and formalin-fixed paraffin-embedded (FFPE, n=46) specimens were included. Fourty-three thyroid cancer-derived cell lines, previously authenticated using short tandem repeat and single nucleotide polymorphism array analysis (54), were also evaluated. Genomic DNA was extracted from all specimens using the DNeasy Tissue kit (Qiagen). Patient samples were studied under a protocol approved by the Memorial Sloan Kettering IRB.

Targeted sequencing and copy number assessment

Two hundred and fifty nanograms of genomic DNA derived from all 126 thyroid samples and matched normal tissues (when available) were subjected to deep-coverage targeted sequencing with MSK-IMPACT™ (Integrated Mutation Profiling of Actionable Cancer Targets), an exon-capture next generation sequencing platform covering the entire coding sequence and intron-exon boundaries of 341 cancer genes(55). Sequence data were analyzed

Author Manuscript Author Manuscript Author Manuscript Author Manuscript

to identify three classes of somatic alterations: single-nucleotide variants, small insertions/deletions (indels), and copy number alterations (CNAs). We focused in greater detail on the six genes mapping on chromosome 22q included in the platform: *CRKL*, *MAPK1*, *SMARCB1*, *CHEK2*, *NF2* and *EP300*.

To confirm the ability of IMPACT to accurately call CNAs, we subjected our subset of 37 frozen tumors to array comparative genomic hybridization (aCGH). Briefly, 3 μg of DNA was digested and labeled by random priming using Cy3 or Cy5-dUTP labeled primers (Invitrogen). Labeled tumor DNA was co-hybridized to Agilent aCGH microarrays with a pool of reference normal DNA for 40 h at 60 °C. After washing, the slides were scanned and images were quantified using Feature Extraction 9.1 (Agilent Technologies). Raw copy-number estimates were normalized and segmented with Circular Binary Segmentation (56). Data were also analyzed using the RAE algorithm(57). IMPACT-sequencing reads and segmented copy-number data from both platforms was visualized in the Integrative Genomics Viewer (58), and all genome coordinates were standardized to NCBI build 37 (hg19) of the reference human genome.

FISH

FISH analysis for *NF2* status was performed by hybridizing a tissue microarray containing 16 ATC specimens with BAC probes for *NF2* probe (RP11-551L12, 22q12.2, red) and *BCR* (22q11.2, green). Deletion of *NF2* was defined as tumors with more than 25% of cells with single or no *NF2* hybridization signals (a minimum of 200 cells were scored for each tumor). This threshold was selected because of the high admixture of stromal cells, particularly tumor-associated macrophages, in these cancers.

Mouse genetic models

TPO-Cre mice express Cre recombinase under the control of the thyroid peroxidase gene promoter, which is active only in thyroid follicular cells beginning at E14.5 (59). *FR-Hras*^{G12V} mice conditionally express a latent *Hras*^{G12V} allele under the regulatory control of its endogenous gene promoter (31). To generate triple transgenic mice *TPO-Cre/FR-Hras* mice were bred with *Nf2*^{flox2} (60), *Trp53*^{flox2} (61), or *Pten*^{flox2} (62). Both male and female mice where used. Mice were in the following backgrounds: *TPO-Cre/FR-Hras*^{G12V}/*Nf2*^{flox2}: ~7 % 129sv, 56% C57bl/6, 12% swiss black, 25% FVB/n; *TPO-Cre/FR-Hras*^{G12V}/*p53*^{flox2}: ~56 % 129sv, 7% C57bl/6, 12% swiss black and 25% FVB/n. *TPO-Cre/FR-Hras*^{G12V}/ *Pten*^{flox2} mice were backcrossed 5 generations into 129sv. *TPO-Cre/FR-Hras*^{G12V}/ *Nf2*^{flox2} and *TPO-Cre/FR-Hras*^{G12V}/ *Pten*^{flox2} mice were treated 5 days a week for 4 weeks with AZD6244 (25 mg/kg/BID) dissolved in 0.1% Tween 80 +0.5% methylcellulose or vehicle. *TPO-Cre/FR-Hras*^{G12V}/ *p53*^{flox2} mice were treated for 7 days a week for 2 weeks. Animal care and all procedures were approved by the MSKCC Institutional Animal Care and Use Committee.

Ultrasound imaging

Mice were anesthetized by inhalation of 2–3% isoflurane with 1% O_2, neck hair removed with defoliating agent and placed on the heated stage. An aqueous ultrasonic gel was applied to the skin overlying the thyroid glands. Thyroid tumors were imaged with the VisualSonics

Author Manuscript Author Manuscript Author Manuscript Author Manuscript

Vevo™ 770 In Vivo High-Resolution Micro-Imaging System (VisualSonics Inc, Toronto, Ontario, Canada). Using the Vevo™ 770 scan module the entire thyroid bed was imaged with captures every 250 microns. Using the instrument's software the volume was calculated by manually tracing the margin of the tumor every 250 microns. The instrument is calibrated to allow measurements to be determined accurately. Animals were included in the study if they had tumor present as demonstrated by ultrasound and at a size that could be accurately measured by the ultrasound probe.

Histology and IHC

Thyroid tissues were immediately placed in 4% paraformaldehyde and incubated overnight at 4°C. The next day, tissue was washed twice with PBS for 30 minutes followed by a single 30-minute 50% ethanol wash. The fixed tissue was then placed in 70% ethanol, paraffin embedded, and sectioned into 4-μm paraffin sections. H&E-stained slides were evaluated by a board-certified pathologist (R. Ghossein). Mouse thyroid sections were deparaffinized and immunostained with an antibody to p-ERK (#9101; Cell Signaling) or $pPAK_{S473}$ (#4051S; Cell Signaling) at the Memorial Sloan-Kettering Cancer Center Molecular Cytology Core Facility.

Thyroid cancer cell lines

Cancer cell lines were maintained at 37°C and 5% CO_2 in humidified atmosphere and grown in RPMI-1640 (C643, Hth83 and Cal62), DMEM (Hth7, ACT1) or DMEM:RPMI (ASH3, KMH2) supplemented with 10% of FBS, 2 mmoL/l glutamine, 50 U/mL penicillin (GIBCO), and 50 μg/mL streptomycin. Cell line C643, Hth7 and Hth83were obtained from Dr. Nils-Erik Heldin on 12/2006, 9/2007 and 12/2006, respectively. Cal62 cells were obtained from Dr. Jeanine Gioanni on 12/2006. The ACT1 line was obtained from Dr. Onoda Osaka in April 2006. ASH3 and KMH2 were obtained from JCRB in April of 2010. All thyroid cancer cell lines used in this study were authenticated using short tandem repeat and single nucleotide polymorphism array analysis between 2006 and 2010 (54). For cell growth assays, cells were plated in triplicate into 6-well plates at 50,000 cells per well, and incubated for 24h. The cells were treated with vehicle or concentrations of the indicated drug in media with 1% of FBS. For transient transfections, 20,000 cells/well were plated into 24-well plates in media containing 10% FBS without antibiotics. 24h after the transfection was performed as indicated in the "Gene Expression and Silencing" Cells were collected by trypsinization and counted in a Vi-Cell series Cell Viability Analyzer (Beckman Coulter) at times indicated. IC_{50} values were calculated by nonlinear regression using Prism v5.04 (GraphPad Software).

Colony formation assay

Cells were seeded in triplicate at 50,000 cells per 35mm dish. Dishes were first coated with a bottom layer of 0.4% agar in RPMI. Cells were resuspended in a top layer of 0.2% agar in RPMI with 10% FBS, and then fed every other day by adding drops of media onto the top layer. After 9 days the colonies were stained with crystal violet and counted in a GelCount™ colony counter (Oxford OPTRONIX). Minimum diameter of the colonies was 50μm.

Author Manuscript Author Manuscript Author Manuscript Author Manuscript

Gene Expression and Silencing

PCR-amplified full length cDNAs of human *NF2 wt* and *NF2-L64P* were cloned into the pLVX-Tight-puro vector (Clontech) using the following primers containing BamHI and EcoRI restriction sites: 5'- GAGAGGATCCTCACCATGGCCGGAGCCATC-3'; 5'-GAGAGAATTCTTCGAACCGCGGGCCCTCTA-3'). Cal62 and Hth83 thyroid cancer cells were co-infected with pLVX-Tight-puro-NF2 or NF2-L64P and with pLVX-tet-on Advanced vector (Clontech). C643 were infected with pLKO.1 and 5 different hairpins for NF2 (M1#TRCN0000039973; M2#TRCN0000039975; M3#TRCN0000039977; M4#TRCN0000010397; M5#TRCN0000018338 from Open Biosystems). For infection, cells were incubated with infectious particles in the presence of 10 ng/ml hexadimethrine bromide (Sigma) overnight. After recovery in complete medium for 24 hours cells were placed under selection in 1μg/ml puromycin or 300μg/ μL G418 for Cal62 and Hth83 or 1μg/ml puromycin for C643. The production of viral particles was performed with Mission Lentiviral Packing mix from SIGMA. Transient transfections were performed using Lipofectamine 2000 (Invitrogen) or Amaxa Nucleofector System (Lonza). Dominant negative of PAK (PAK1 83–149) and YAP1-S127A were purchased from Addgene (#17790, #12214 respectively) (63, 64). Short interfering RNAs for YAP were from ORIGENE (SR307060). The media (10% FBS without antibiotics) was changed 4–6 hours after transfection. Efficiency of knockdown or overexpression was verified by immunoblotting.

RNA isolation, cDNA synthesis and qPCR

Total mRNA from snap frozen thyroid tissue was extracted with the PrepEase Kit (USB Corporation); total mRNA from cells was isolated by Trizol (Invitrogen). Equal amounts of isolated RNA (2μg) were subjected to DNase I Amplification Grade (Invitrogen) and subsequently reverse transcribed into cDNA using the SuperScript® III Reverse Transcriptase (Invitrogen) according to the manufacturer's instructions. qPCR was then performed with the Power SYBR Green PCR Master Mix (Applied Biosystems). See Supplemental Table 3 for list of primers used. Expression was analyzed with the ΔΔCt method. The Ct values of the target genes were normalized to that of the housekeeping genes beta actin or GAPDH.

Hras allelic imbalance analysis

Genomic DNA from mouse thyroid tissues was used as template for PCR amplification with primers that distinguish mutant (668 bp product due to insertion of *loxp*) from WT-*Hras* alleles (622 bp). The primers and PCR conditions were previously described (31).

mRNA stability

Cells were treated with 1 μM actinomycin D for 1, 3, 6, 12 and 24 hours prior to harvesting. The mRNA levels were measured by quantitative RT-PCR using Power SYBR Green PCR Master Mix (Applied Biosystems).

Author Manuscript Author Manuscript Author Manuscript Author Manuscript

Immunoblotting

Cells were washed twice with cold PBS and lysed in lysis buffer (containing 125mM HEPES, pH7.5, 750mM NaCl, 5% Igepal CA-630, 50mM $MgCl_2$, 5mM EDTA and 10% glycerol) supplemented with proteinase and phosphatase inhibitors (Roche). Protein concentration was determined using the BCA kit (Thermo Scientific). Western blots were conducted on 20 μg protein separated by 4–12% Bis-Tris SDS-PAGE gels (Invitrogen), transferred to PVDF membranes, and immunoblotted after blocking with 5% skim milk with the corresponding primary antibodies (listed below) in 5% BSA (SIGMA). This was followed by incubation for 1h with secondary antibodies conjugated with goat anti-rabbit HRP-conjugated antibody (1:5,000; Santa Cruz sc-2054) or goat anti-mouse HRP-conjugated antibody (1:5,000; Santa Cruz sc-2005). Bound antibodies were detected by chemiluminescence with the ECL detection system (GE Healthcare Biosciences).

RAS-GTP or RAC1-GTP immunoprecipitation was conducted using the RAS or RAC1 activation assay kits, respectively, from Millipore, according to the manufacturer's protocol and subjected to Western blotting with the indicated antibodies. Cells were treated during 72h with dox in media with 1% of FBS.

Subcellular fractions were prepared using the Subcellular Protein Fractionation Kit for cultured cells following the manufacturer’s instructions (Thermo Fisher Scientific). Fractions were subjected to Western blotting with the indicated antibodies.

Chromatin Immunoprecipitation

Chromatin immunoprecipitation (ChIP) lysates isolated from Cal62, Hth83 and C643 cells were cross-linked with 1% formaldehyde for 10 minutes at room temperature, and stopped by the addition of glycine to a final concentration of 125 mmol/L followed by 2 washes with PBS. The cell pellet was resuspended in Lysis buffer (ChIP-IT® Express Enzymatic kit - Active Motif) supplemented with PMSF and protease inhibitors and incubated on ice for 30 minutes. After 20 strokes with a homogenizer and a centrifugation for 10 minutes at 5000rpm, the pellets were digested with an enzymatic shearing cocktail for 7 minutes at 37°C, to produce chromatin fragments of 200–500 bp on average. Equal amounts of cross-linked DNA were immunoprecipated overnight at 4°C with antibodies against YAP (sc-15407, Santa Cruz) or TEAD1 (#8526, Cell Signaling). Immunoprecipates were incubated with proteinase K overnight, and the DNA recovered by purification (QIAquick PCR purification kit from Quiagen) prior to real time PCR with primers bracketing the indicated promoter motifs. The ChIP ratio was calculated as enrichment over noise normalized to input.

Additional reagents used *in vitro*

Doxycycline (2μg/mL), hEGF (5ng/mL) and verteporfin were from Sigma. AZD6244 was from AstraZeneca. FRAX597 was from Selleckchem.

Statistical Analysis

Statistical analyses of the results were performed by unpaired two tailed Student's *t* test or Mann-Whitney test according to assumptions of the test, using Prism v5.04 (GraphPad

Author Manuscript Author Manuscript Author Manuscript Author Manuscript

Software). Graphs represent mean value and error bars represents s.d. Similar variance between groups was tested by F Test; if different, Welch's correction was applied. The *P* values are presented in figure legends where p< 5 × E-2 was considered statistically significant. No randomization or blinding was used.

Antibodies

pMEK S217/221 (9121L), pERK (#4376), CCND1 (#2978P), pYAP S127 (#4911), YAP/TAZ (#8418), TUBULIN (#2148), pPAK T423 (#2601), PAK (#2604S), pCRAF s338 (#9427), pMEK S298 (#9128), pEGFR Y1068 (#3777S), EGFR (#4267S), GST (#2622), TEAD1 (#8526), FLAG (#2368S) from Cell Signaling; NF2/MERLIN ((a-19) sc-331), HRAS (sc-520), KRAS (sc-30), NRAS (sc-31), CTGF (sc-14939), YAP FOR ChIP (sc-15407) from Santa Cruz; ACTIN (A2228), pPAK S141 (p7871) from Sigma; Na+K+ ATPase (ab818), TATA binding (ab7671) from Abcam.

Supplementary Material

Refer to Web version on PubMed Central for supplementary material.

Acknowledgements

We thank the Molecular Cytology, Comparative Pathology, Animal Imaging and the Mouse Genetics Core Facilities for support of this project.

Grant support

This work was supported, in part, by NIH grants CA50706, CA72597, P50-CA72012 and P30-CA008748, the Margot Rosenberg Pulitzer and the Lefkovsky Family Foundations, the Society of Memorial Sloan Kettering and the Byrne fund.

Reference List

1. Rouleau GA, Merel P, Lutchman M, Sanson M, Zucman J, Marineau C, et al. Alteration in a new gene encoding a putative membrane-organizing protein causes neuro-fibromatosis type 2. Nature. 1993; 363:515–521. [PubMed: 8379998]
2. Hamaratoglu F, Willecke M, Kango-Singh M, Nolo R, Hyun E, Tao C, et al. The tumour-suppressor genes NF2/Merlin and Expanded act through Hippo signalling to regulate cell proliferation and apoptosis. Nat Cell Biol. 2006; 8:27–36. [PubMed: 16341207]
3. Curto M, McClatchey AI. Nf2/Merlin: a coordinator of receptor signalling and intercellular contact. Br J Cancer. 2008; 98:256–262. [PubMed: 17971776]
4. Curto M, Cole BK, Lallemand D, Liu CH, McClatchey AI. Contact-dependent inhibition of EGFR signaling by Nf2/Merlin. J Cell Biol. 2007; 177:893–903. [PubMed: 17548515]
5. Shaw RJ, Paez JG, Curto M, Yaktine A, Pruitt WM, Saotome I, et al. The Nf2 tumor suppressor, merlin, functions in Rac-dependent signaling. Dev Cell. 2001; 1:63–72. [PubMed: 11703924]
6. Sherman LS, Gutmann DH. Merlin: hanging tumor suppression on the Rac. Trends Cell Biol. 2001; 11:442–444. [PubMed: 11684412]
7. Yi C, Wilker EW, Yaffe MB, Stemmer-Rachamimov A, Kissil JL. Validation of the p21-activated kinases as targets for inhibition in neurofibromatosis type 2. Cancer Res. 2008; 68:7932–7937. [PubMed: 18829550]
8. James MF, Han S, Polizzano C, Plotkin SR, Manning BD, Stemmer-Rachamimov AO, et al. NF2/merlin is a novel negative regulator of mTOR complex 1, and activation of mTORC1 is associated with meningioma and schwannoma growth. Mol Cell Biol. 2009; 29:4250–4261. [PubMed: 19451225]

Author Manuscript Author Manuscript Author Manuscript Author Manuscript

9. Lopez-Lago MA, Okada T, Murillo MM, Socci N, Giancotti FG. Loss of the tumor suppressor gene NF2, encoding merlin, constitutively activates integrin-dependent mTORC1 signaling. Mol Cell Biol. 2009; 29:4235–4249. [PubMed: 19451229]
10. Li W, You L, Cooper J, Schiavon G, Pepe-Caprio A, Zhou L, et al. Merlin/NF2 suppresses tumorigenesis by inhibiting the E3 ubiquitin ligase CRL4(DCAF1) in the nucleus. Cell. 2010; 140:477–490. %19. [PubMed: 20178741]
11. Zhang H, Liu CY, Zha ZY, Zhao B, Yao J, Zhao S, et al. TEAD transcription factors mediate the function of TAZ in cell growth and epithelial-mesenchymal transition. J Biol Chem. 2009; 284:13355–13362. [PubMed: 19324877]
12. Zhao B, Ye X, Yu J, Li L, Li W, Li S, et al. TEAD mediates YAP-dependent gene induction and growth control. Genes Dev. 2008; 22:1962–1971. [PubMed: 18579750]
13. Dong J, Feldmann G, Huang J, Wu S, Zhang N, Comerford SA, et al. Elucidation of a universal size-control mechanism in Drosophila and mammals. Cell. 2007; 130:1120–1133. [PubMed: 17889654]
14. Liu-Chittenden Y, Huang B, Shim JS, Chen Q, Lee SJ, Anders RA, et al. Genetic and pharmacological disruption of the TEAD-YAP complex suppresses the oncogenic activity of YAP. Genes Dev. 2012; 26:1300–1305. [PubMed: 22677547]
15. Harvey KF, Zhang X, Thomas DM. The Hippo pathway and human cancer. Nat Rev Cancer. 2013; 13:246–257. [PubMed: 23467301]
16. Iyer G, Hanrahan AJ, Milowsky MI, Al-Ahmadie H, Scott SN, Janakiraman M, et al. Genome sequencing identifies a basis for everolimus sensitivity. Science. 2012; 338:221. [PubMed: 22923433]
17. Houshmandi SS, Emnett RJ, Giovannini M, Gutmann DH. The neurofibromatosis 2 protein, merlin, regulates glial cell growth in an ErbB2- and Src-dependent manner. Mol Cell Biol. 2009; 29:1472–1486. [PubMed: 19103750]
18. Zhang N, Bai H, David KK, Dong J, Zheng Y, Cai J, et al. The Merlin/NF2 tumor suppressor functions through the YAP oncoprotein to regulate tissue homeostasis in mammals. Dev Cell. 2010; 19:27–38. %20. [PubMed: 20643348]
19. Benhamouche S, Curto M, Saotome I, Gladden AB, Liu CH, Giovannini M, et al. Nf2/Merlin controls progenitor homeostasis and tumorigenesis in the liver. Genes Dev. 2010; 24:1718–1730. [PubMed: 20675406]
20. Kimura ET, Nikiforova MN, Zhu Z, Knauf JA, Nikiforov YE, Fagin JA. High prevalence of BRAF mutations in thyroid cancer: genetic evidence for constitutive activation of the RET/PTC-RAS-BRAF signaling pathway in papillary thyroid carcinoma. Cancer Res. 2003; 63:1454–1457. [PubMed: 12670889]
21. Volante M, Rapa I, Gandhi M, Bussolati G, Giachino D, Papotti M, et al. RAS mutations are the predominant molecular alteration in poorly differentiated thyroid carcinomas and bear prognostic impact. J Clin Endocrinol Metab. 2009; 94:4735–4741. [PubMed: 19837916]
22. Ricarte-Filho JC, Ryder M, Chitale DA, Rivera M, Heguy A, Ladanyi M, et al. Mutational profile of advanced primary and metastatic radioactive iodine-refractory thyroid cancers reveals distinct pathogenetic roles for BRAF, PIK3CA, and AKT1. Cancer Res. 2009; 69:4885–4893. [PubMed: 19487299]
23. Smallridge RC, Marlow LA, Copland JA. Anaplastic thyroid cancer: molecular pathogenesis and emerging therapies. Endocr Relat Cancer. 2009; 16:17–44. [PubMed: 18987168]
24. Cancer Genome Research Atlas Network. Cell. 2014; 159:676–680. [PubMed: 25417114]
25. Zucman-Rossi J, Legoix P, Der SH, Cheret G, Sor F, Bernardi A, et al. NF2 gene in neurofibromatosis type 2 patients. Hum Mol Genet. 1998; 7:2095–2101. [PubMed: 9817927]
26. Lepont P, Stickney JT, Foster LA, Meng JJ, Hennigan RF, Ip W. Point mutation in the NF2 gene of HEI-193 human schwannoma cells results in the expression of a merlin isoform with attenuated growth suppressive activity. Mutat Res. 2008; 637:142–151. [PubMed: 17868749]
27. Serrano I, McDonald PC, Lock F, Muller WJ, Dedhar S. Inactivation of the Hippo tumour suppressor pathway by integrin-linked kinase. Nat Commun. 2013; 4:2976. [PubMed: 24356468]

Author Manuscript Author Manuscript Author Manuscript Author Manuscript

28. Bianchi AB, Hara T, Ramesh V, Gao J, Klein-Szanto AJ, Morin F, et al. Mutations in transcript isoforms of the neurofibromatosis 2 gene in multiple human tumour types. Nat Genet. 1994; 6:185–192. [PubMed: 8162073]
29. Yang C, Asthagiri AR, Iyer RR, Lu J, Xu DS, Ksendzovsky A, et al. Missense mutations in the NF2 gene result in the quantitative loss of merlin protein and minimally affect protein intrinsic function. Proc Natl Acad Sci U S A. 2011; 108:4980–4985. [PubMed: 21383154]
30. Kimura Y, Koga H, Araki N, Mugita N, Fujita N, Takeshima H, et al. The involvement of calpain-dependent proteolysis of the tumor suppressor NF2 (merlin) in schwannomas and meningiomas. Nat Med. 1998; 4:915–922. [PubMed: 9701243]
31. Chen X, Mitsutake N, LaPerle K, Akeno N, Zanzonico P, Longo VA, et al. Endogenous expression of Hras(G12V) induces developmental defects and neoplasms with copy number imbalances of the oncogene. Proc Natl Acad Sci U S A. 2009; 106:7979–7984. [PubMed: 19416908]
32. Bashour AM, Meng JJ, Ip W, MacCollin M, Ratner N. The neurofibromatosis type 2 gene product, merlin, reverses the F-actin cytoskeletal defects in primary human Schwannoma cells. Mol Cell Biol. 2002; 22:1150–1157. [PubMed: 11809806]
33. Yi C, Troutman S, Fera D, Stemmer-Rachamimov A, Avila JL, Christian N, et al. A tight junction-associated Merlin-angiomotin complex mediates Merlin's regulation of mitogenic signaling and tumor suppressive functions. Cancer Cell. 2011; 19:527–540. [PubMed: 21481793]
34. Michels S, Schmidt-Erfurth U. Photodynamic therapy with verteporfin: a new treatment in ophthalmology. Semin Ophthalmol. 2001; 16:201–206. [PubMed: 15513441]
35. Finney RE, Bishop JM. Predisposition to neoplastic transformation caused by gene replacement of H-ras1. Science. 1993; 260:1524–1527. [PubMed: 8502998]
36. Bremner R, Balmain A. Genetic changes in skin tumor progression: correlation between presence of a mutant ras gene and loss of heterozygosity on mouse chromosome 7. Cell. 1990; 61:407–417. [PubMed: 2185890]
37. Chen X, Makarewicz JM, Knauf JA, Johnson LK, Fagin JA. Transformation by Hras is consistently associated with mutant allele copy gains and is reversed by farnesyl transferase inhibition. Oncogene. 2013:10.
38. Xu J, Haigis KM, Firestone AJ, McNerney ME, Li Q, Davis E, et al. Dominant role of oncogene dosage and absence of tumor suppressor activity in Nras-driven hematopoietic transformation. Cancer Discov. 2013; 3:993–1001. [PubMed: 23733505]
39. Namba H, Gutman RA, Matsuo K, Alvarez A, Fagin JA. H-ras protooncogene mutations in human thyroid neoplasms. J Clin Endocrinol Metab. 1990; 71:223–229. [PubMed: 2196280]
40. Johnson SM, Grosshans H, Shingara J, Byrom M, Jarvis R, Cheng A, et al. RAS is regulated by the let-7 microRNA family. Cell. 2005; 120:635–647. [PubMed: 15766527]
41. Johnson CD, Esquela-Kerscher A, Stefani G, Byrom M, Kelnar K, Ovcharenko D, et al. The let-7 microRNA represses cell proliferation pathways in human cells. Cancer Res. 2007; 67:7713–7722. [PubMed: 17699775]
42. Kumar MS, Erkeland SJ, Pester RE, Chen CY, Ebert MS, Sharp PA, et al. Suppression of non-small cell lung tumor development by the let-7 microRNA family. Proc Natl Acad Sci U S A. 2008; 105:3903–3908. [PubMed: 18308936]
43. Lamar JM, Stern P, Liu H, Schindler JW, Jiang ZG, Hynes RO. The Hippo pathway target, YAP, promotes metastasis through its TEAD-interaction domain. Proc Natl Acad Sci U S A. 2012; 109:E2441–E2450. [PubMed: 22891335]
44. Xie Q, Chen J, Feng H, Peng S, Adams U, Bai Y, et al. YAP/TEAD-mediated transcription controls cellular senescence. Cancer Res. 2013; 73:3615–3624. [PubMed: 23576552]
45. Lee KP, Lee JH, Kim TS, Kim TH, Park HD, Byun JS, et al. The Hippo-Salvador pathway restrains hepatic oval cell proliferation, liver size, and liver tumorigenesis. Proc Natl Acad Sci U S A. 2010; 107:8248–8253. [PubMed: 20404163]
46. Lu L, Li Y, Kim SM, Bossuyt W, Liu P, Qiu Q, et al. Hippo signaling is a potent in vivo growth and tumor suppressor pathway in the mammalian liver. Proc Natl Acad Sci U S A. 2010; 107:1437–1442. [PubMed: 20080689]
47. Urtasun R, Latasa MU, Demartis MI, Balzani S, Goni S, Garcia-Irigoyen O, et al. Connective tissue growth factor autocriny in human hepatocellular carcinoma: oncogenic role and regulation

Author Manuscript Author Manuscript Author Manuscript Author Manuscript

by epidermal growth factor receptor/yes-associated protein-mediated activation. Hepatology. 2011; 54:2149–2158. [PubMed: 21800344]

48. Kapoor A, Yao W, Ying H, Hua S, Liewen A, Wang Q, et al. Yap1 activation enables bypass of oncogenic Kras addiction in pancreatic cancer. Cell. 2014; 158:185–197. [PubMed: 24954535]
49. Shao DD, Xue W, Krall EB, Bhutkar A, Piccioni F, Wang X, et al. KRAS and YAP1 converge to regulate EMT and tumor survival. Cell. 2014; 158:171–184. [PubMed: 24954536]
50. Zhang W, Nandakumar N, Shi Y, Manzano M, Smith A, Graham G, et al. Downstream of Mutant KRAS, the Transcription Regulator YAP Is Essential for Neoplastic Progression to Pancreatic Ductal Adenocarcinoma. Sci Signal. 2014; 7:ra42. [PubMed: 24803537]
51. Lian I, Kim J, Okazawa H, Zhao J, Zhao B, Yu J, et al. The role of YAP transcription coactivator in regulating stem cell self-renewal and differentiation. Genes Dev. 2010; 24:1106–1118. [PubMed: 20516196]
52. McClatchey AI, Saotome I, Mercer K, Crowley D, Gusella JF, Bronson RT, et al. Mice heterozygous for a mutation at the Nf2 tumor suppressor locus develop a range of highly metastatic tumors. Genes Dev. 1998; 12:1121–1133. [PubMed: 9553042]
53. Manchanda PK, Jones GN, Lee AA, Pringle DR, Zhang M, Yu L, et al. Rac1 is required for Prkar1a–mediated Nf2 suppression in Schwann cell tumors. Oncogene. 2013; 32:3491–3499. [PubMed: 23045281]
54. Schweppe RE, Klopper JP, Korch C, Pugazhenthi U, Benezra M, Knauf JA, et al. Deoxyribonucleic acid profiling analysis of 40 human thyroid cancer cell lines reveals cross-contamination resulting in cell line redundancy and misidentification. J Clin Endocrinol Metab. 2008; 93:4331–4341. [PubMed: 18713817]
55. Won HH, Scott SN, Brannon AR, Shah RH, Berger MF. Detecting somatic genetic alterations in tumor specimens by exon capture and massively parallel sequencing. J Vis Exp. 2013:e50710. [PubMed: 24192750]
56. Venkatraman ES, Olshen AB. A faster circular binary segmentation algorithm for the analysis of array CGH data. Bioinformatics. 2007; 23:657–663. [PubMed: 17234643]
57. Taylor BS, Barretina J, Socci ND, Decarolis P, Ladanyi M, Meyerson M, et al. Functional copy-number alterations in cancer. PLoS ONE. 2008; 3:e3179. [PubMed: 18784837]
58. Robinson JT, Thorvaldsdottir H, Winckler W, Guttman M, Lander ES, Getz G, et al. Integrative genomics viewer. Nat Biotechnol. 2011; 29:24–26. [PubMed: 21221095]
59. Kusakabe T, Kawaguchi A, Kawaguchi R, Feigenbaum L, Kimura S. Thyrocyte-specific expression of Cre recombinase in transgenic mice. Genesis. 2004; 39:212–216. [PubMed: 15282748]
60. Giovannini M, Robanus-Maandag E, van dV, Niwa-Kawakita M, Abramowski V, Goutebroze L, et al. Conditional biallelic Nf2 mutation in the mouse promotes manifestations of human neurofibromatosis type 2. Genes Dev. 2000; 14:1617–1630. [PubMed: 10887156]
61. Jonkers J, Meuwissen R, van der Gulden H, Peterse H, van dV, Berns A. Synergistic tumor suppressor activity of BRCA2 and p53 in a conditional mouse model for breast cancer. Nat Genet. 2001; 29:418–425. [PubMed: 11694875]
62. Trotman LC, Niki M, Dotan ZA, Koutcher JA, Di CA, Xiao A, et al. Pten dose dictates cancer progression in the prostate. PLoS Biol. 2003; 1:E59. [PubMed: 14691534]
63. Xiao GH, Beeser A, Chernoff J, Testa JR. p21-activated kinase links Rac/Cdc42 signaling to merlin. J Biol Chem. 2002; 277:883–886. [PubMed: 11719502]
64. Overholtzer M, Zhang J, Smolen GA, Muir B, Li W, Sgroi DC, et al. Transforming properties of YAP, a candidate oncogene on the chromosome 11q22 amplicon. Proc Natl Acad Sci U S A. 2006; 103:12405–12410. [PubMed: 16894141]

Author Manuscript Author Manuscript Author Manuscript Author Manuscript

Significance

Intensification of mutant Ras signaling through copy-number imbalances is commonly associated with transformation. We show that NF2/merlin inactivation augments mutant RAS signaling by promoting YAP/TEAD-driven transcription of oncogenic and wild-type RAS, resulting in greater MAPK output and increased sensitivity to MEK inhibitors.

Author Manuscript Author Manuscript Author Manuscript Author Manuscript

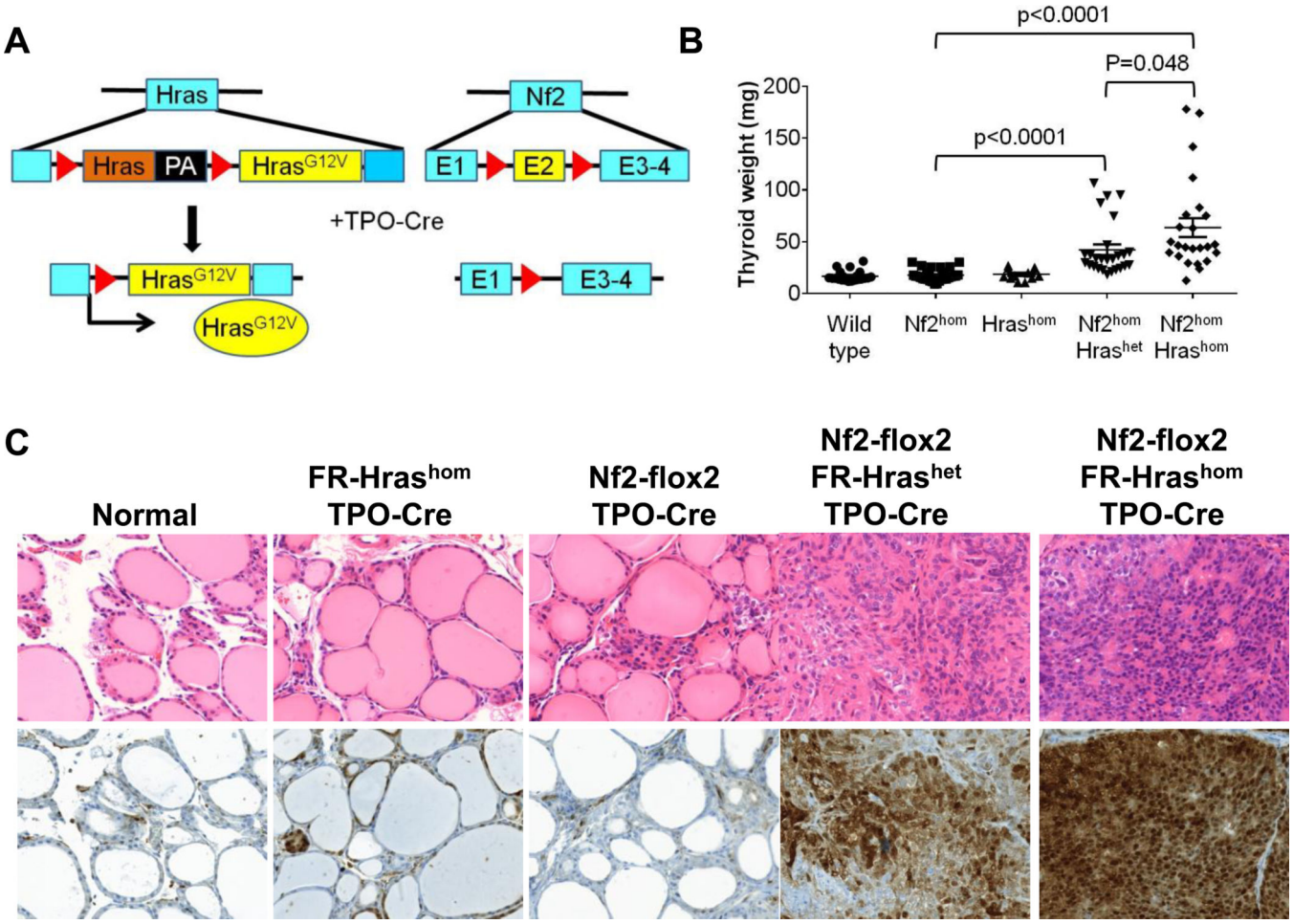

Figure 1. TPO-Cre/FR-Hras^{G12V}/Nf2^{flox2} mice develop poorly differentiated thyroid cancers with strong activation of MAPK signaling

A) *Left*: The *Hras* allele in *FR-Hras^{G12V}* mice is replaced with 2 tandem copies of the gene, the first encoding *WT Hras* flanked by loxP sites, and the second harboring a mutation encoding Hras^{G12V}, which is only expressed after *Cre* excision of the floxed WT allele. *Right*: Exon 2 of *Nf2* is floxed in *Nf2^{flox2}* mice. Thyroid-specific expression of *Hras^{G12V}* and inactivation of *Nf2* was achieved by crosses with *TPO-Cre* mice.

B) Weight of thyroids in 18 month-old mice with the indicated genotype (p values calculated by unpaired t test with Welch's correction).

C) H&E-stained and pERK IHC thyroid sections representative of each genotype. The histology of tumors in *Hras^{G12V}/Nf2^{flox2}* mice is consistent with PDTC.

The mouse age was from 74–85 weeks for *TPO-Cre/FR-Hras^{G12V}/Nf2^{flox2}* (hets: n=23; hom: n=20) and *TPO-Cre/FR-Hras^{G12V}* (hom: n=8). *TPO-Cre* (n=21) and *TPO-Cre/Nf2^{flox2}* (n=27) were 77–119 weeks old.

Author Manuscript Author Manuscript Author Manuscript Author Manuscript

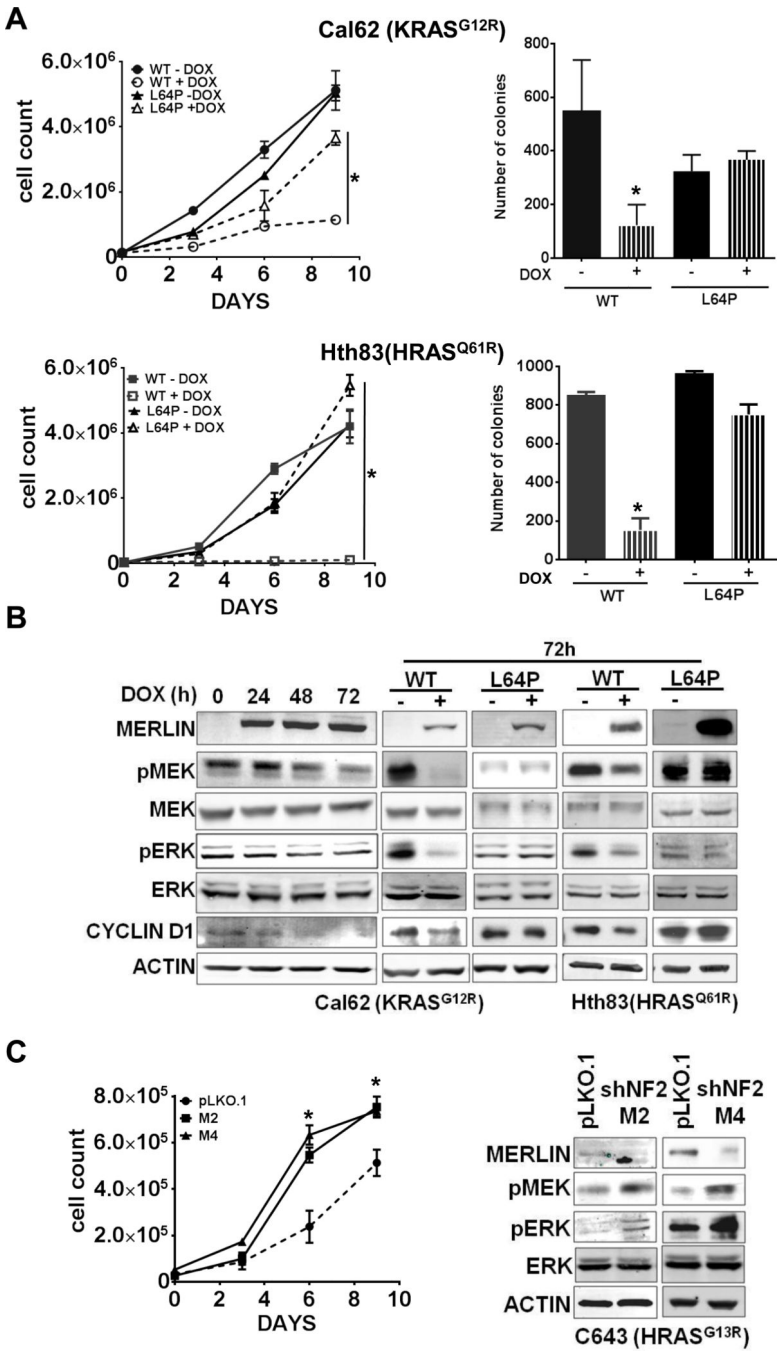

Figure 2. Merlin inhibits growth and MAPK signaling in RAS mutant thyroid cancer cells

A) *Left:* Effects of dox-induced expression of WT NF2 or NF2-L64P on growth of Cal62 ($KRAS^{G12R}$) and Hth83 ($HRAS^{Q61R}$) cells (*p<4 × E-4, dox-induced WT NF2 versus NF2-L64P; n=3, Student's *t* test). *Right:* Soft agar colony counts of Cal62 and Hth83 cells treated with or without dox for 20 days, with media changes every 2 days (*p< 2 × E-2; **p< 1 × E-3; n=3, Student's *t* test).

Author Manuscript Author Manuscript Author Manuscript Author Manuscript

B) *Left:* Time course of MAPK signaling after dox-induced merlin expression in Cal62 cells. *Right:* Effect of dox-induced expression of wild type or L64P–NF2 after 72 h in Cal62 and Hth83 cells.

C) *Left:* Growth of C643 cells (*HRAS*^{G13R}*NF2-WT*) stably expressing scrambled or 2 different NF2 shRNAs (M2 and M4) (*p< 1 × E-3; n=3, Student's *t* test). *Right:* Western blots for pMEK and pERK after NF2 knockdown.

Author Manuscript Author Manuscript Author Manuscript Author Manuscript

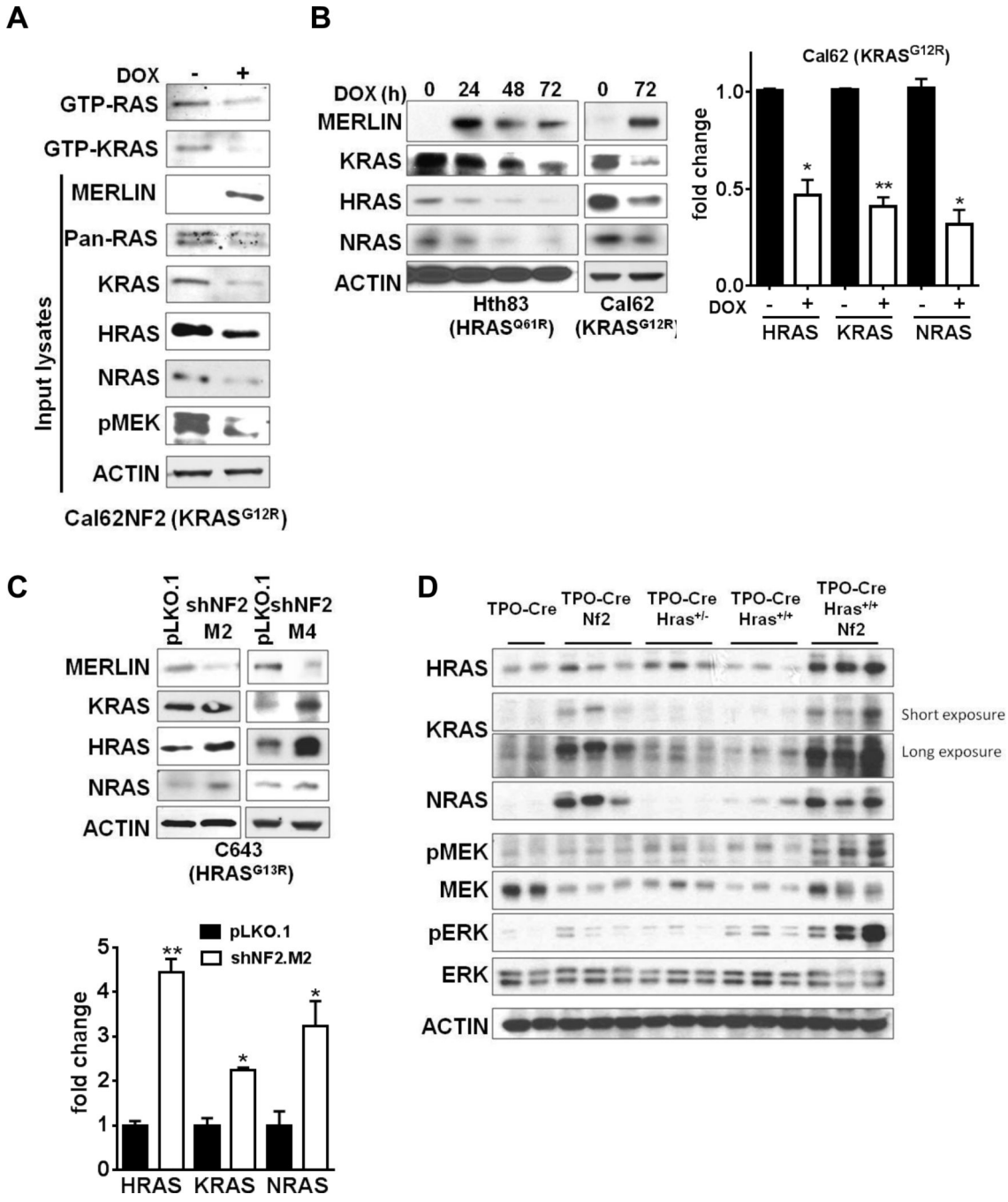

Figure 3. Merlin decreases RAS gene expression and total and oncogenic RAS-GTP levels

A) Total RAS-GTP and KRAS-GTP levels of Cal62 (*KRAS*^{G12R}) cells before and 72h after induction of merlin. Input lysates were blotted for the indicated proteins. No GTP-bound NRAS or HRAS was detected (not shown).

B) *Left:* Oncogenic and wild type RAS protein levels in Cal62 (*KRAS*^{G12R}) and Hth83 (*HRAS*^{Q61R}) cells after merlin expression. *Right:* Merlin decreases mRNA levels of the three RAS genes as measured by real time PCR (*p<2 × E-3; ** p<3 × E-4; Student's *t* test).

Author Manuscript Author Manuscript Author Manuscript Author Manuscript

C) *Top:* shRNA knockdown of NF2 with two different hairpins (M2 and M4) increases RAS protein levels in C643 (*HRAS*^{G13R}-NF2 WT) cells. *Bottom:* Knockdown of NF2 (shNF2.M2) increases RAS mRNAs in C643 cells (*p<5 × E-2, **p<4 × E-4; Student's *t* test).

D) Western blots of thyroid tissues of *TPO-CreTPO-Cre/Nf2*^{flox2}*TPO-Cre/ Hras*$^{G12V+/-}$*(heterozygous), TPO-Cre/Hras*$^{G12V+/+}$ *(homozygous)* and *TPO-Cre/ Hras*$^{G12V+/+}$*/Nf2*^{flox2} mice probed with the indicated antibodies. Each lane contained pooled thyroids, except where indicated. *TPO-Cre*: pool of 4 thyroids each from 12–15 week-old mice; *TPO-Cre/Nf2*^{flox2} pools of two thyroids each from 101–115 week-old mice; *TPO-Cre/ Hras*$^{G12V+/-}$: pools of two thyroids each from 10 week-old mice; *TPO-Cre/Hras*$^{G12V+/+}$: single thyroids and *TPO-Cre/ Hras*^{G12V}*/Nf2*^{flox2}: pools of two thyroids, 66–79 weeks old.

Author Manuscript Author Manuscript Author Manuscript Author Manuscript

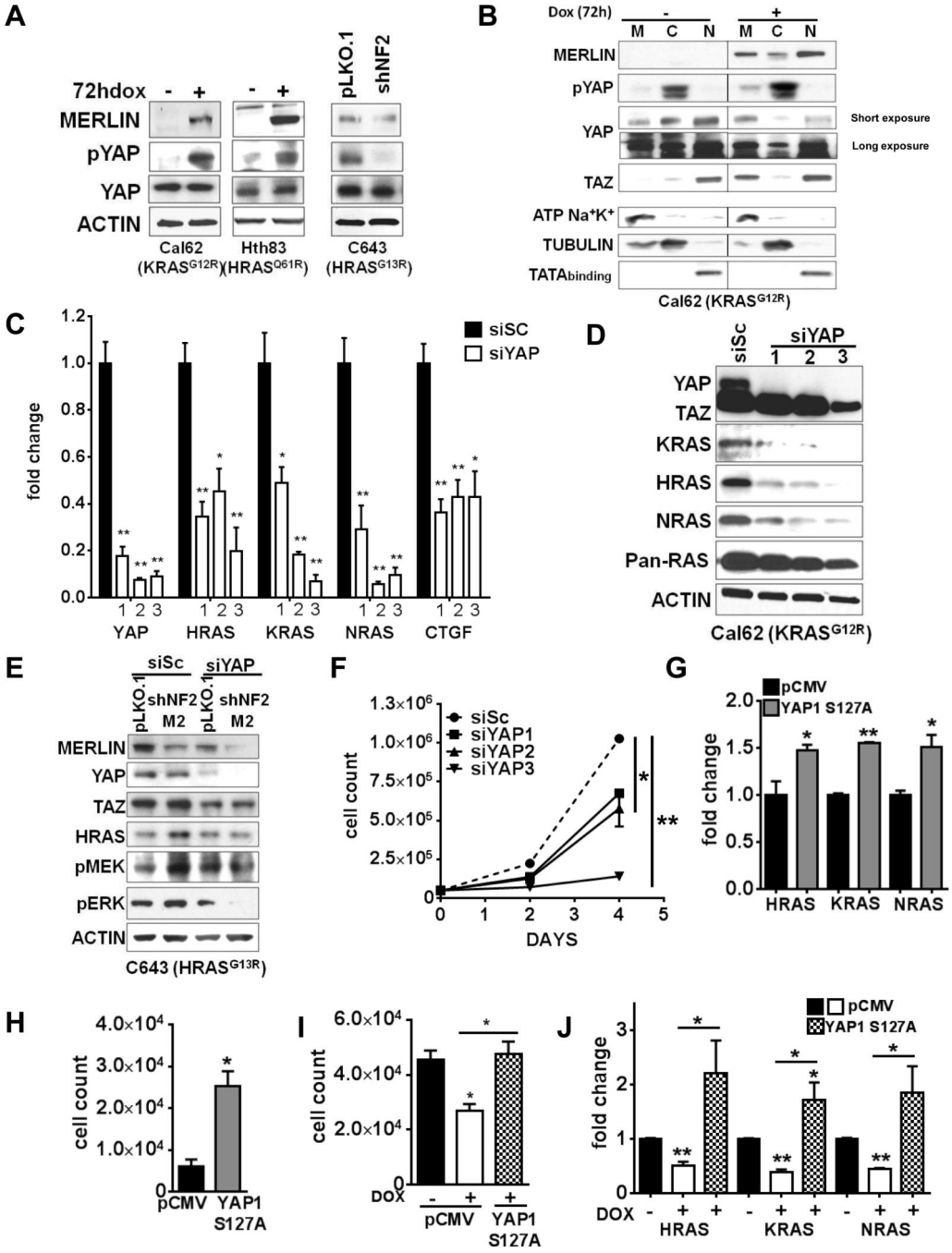

Figure 4. Merlin loss increases RAS gene and protein expression through YAP

A) *Left:* Dox-induction of merlin increases YAP phosphorylation in Cal62 (*KRAS*^{G12R}) and Hth83 (*HRAS*^{Q61R}) NF2 null cells. *Right:* Merlin knockdown decreases pYAP in C643 (*HRAS*^{G13R}-NF2-WT) cells.

B) Western blots of subcellular protein fractions of Cal62 (*KRAS*^{G12R}) lysates treated with or without dox for 72h. M: membrane. C: cytoplasm. N: nucleus. Controls were: M: Na^+K^+ ATPase; C: Tubulin. N: TATA binding protein.

Author Manuscript Author Manuscript Author Manuscript Author Manuscript

C) RT-PCR for the indicated transcripts in Cal62 cells expressing three different siRNAs for YAP (1, 2 and 3) or a scrambled siRNA (siSC) (*p<2 × E-3; **p<1 × E-4; Holm-Sidak method). Bars represent the average of 4 independent experiments. **D)** Western blot of Cal62 cell lysates with the indicted antibodies 72 h after transfection with siSC or YAP siRNAs. The antibody to YAP recognizes both YAP and TAZ.

E) C643 cells stably expressing shNF2.M2 have increased expression of HRAS and higher pMEK and pERK, which is abolished in cells transfected with YAP siRNA.

F) Growth of Cal62 cells expressing scrambled or YAP siRNAs. Cells were incubated in 10% serum and counted 4 days after transfection (*p < 3 × E-3, **p < 1 × E-6; n=3, Student's t test).

G) $Yap1^{S127A}$ increases RAS mRNA levels in C643 cells (*p < 5 × E-2; ** p < 6 × E-4; Student's *t* test).

H) Transient expression of constitutively active $Yap1^{S127A}$ induces C643 cell growth. Bars represent cell counts at 6 days (p< 8 × E-3; Student's *t* test).

I) $Yap1^{S127A}$ rescues the inhibition of growth (p < 2 × E-3; Student's *t* test) and **(J)** of RAS mRNA (* p < 5 × E-2; ** p < 3 × E-3; Student's *t* test) by dox-induced merlin in Cal62 cells.

Author Manuscript
Author Manuscript
Author Manuscript
Author Manuscript

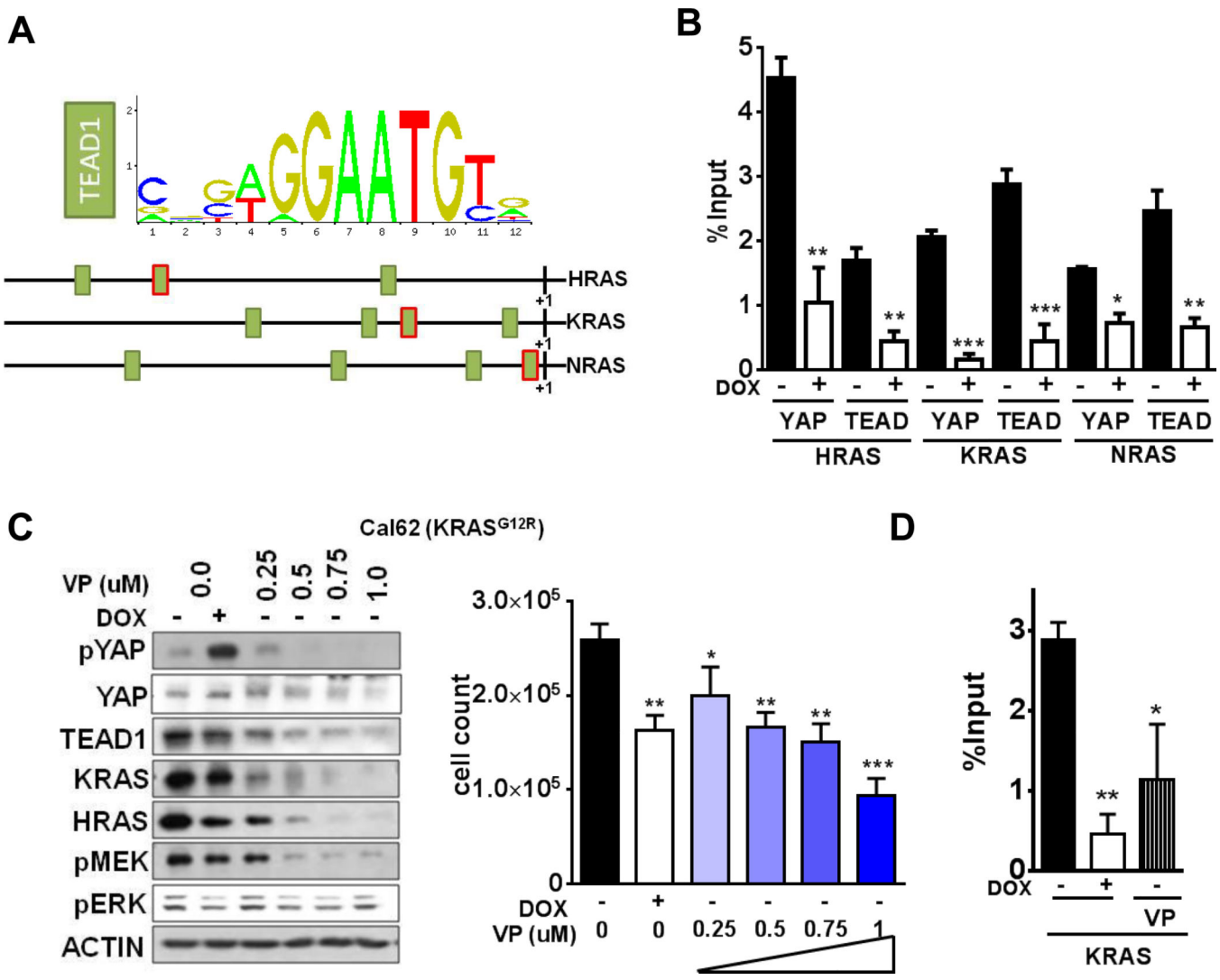

Figure 5. Merlin loss increases RAS gene expression through YAP/TEAD-dependent transcriptional activation

A) Putative TEAD binding motifs in the three *RAS* gene promoters. Highlighted in red are the binding sites shown in the ChiP figure.

B) Merlin decreases YAP and TEAD promoter occupancy of *RAS* gene promoters. ChIP-PCR with antibodies to YAP and TEAD1 in Cal62 cells treated with or without dox for 72h (*p < 3 × E-2; ** p< 7 × E-3; *** p< 2 × E-4; n=3, three independent experiments, Student's *t* test). Primers used bracketed consensus TEAD binding sites in the 3 *RAS* genes (highlighted in red in panel A).

C) *Left:* Dose-dependent decrease of YAP, pYAP and TEAD by 72h of incubation with verteporfin (VP) in Cal62 cells is associated with lower KRAS and HRAS, and decreased pMEK and pERK signaling. Control cells were treated with dox for 72h. *Right:* VP decreases growth of Cal62 cells in a dose-dependent manner. Cells were counted 3 days after incubation with the indicated concentration of the compound (*p < 5 × E-2; ** p< 3 × E-3; *** p< 4 × E-4; n=3).

Author Manuscript Author Manuscript Author Manuscript Author Manuscript

D) ChIP-PCR with TEAD antibody for KRAS in Cal62 cells treated with or without dox in the presence or absence of 0.5uM of VP for 72h (* p< 2 × E-3; ** p< 4 × E-4; n=3, three independent experiments, Student's *t*).

Author Manuscript
Author Manuscript
Author Manuscript
Author Manuscript

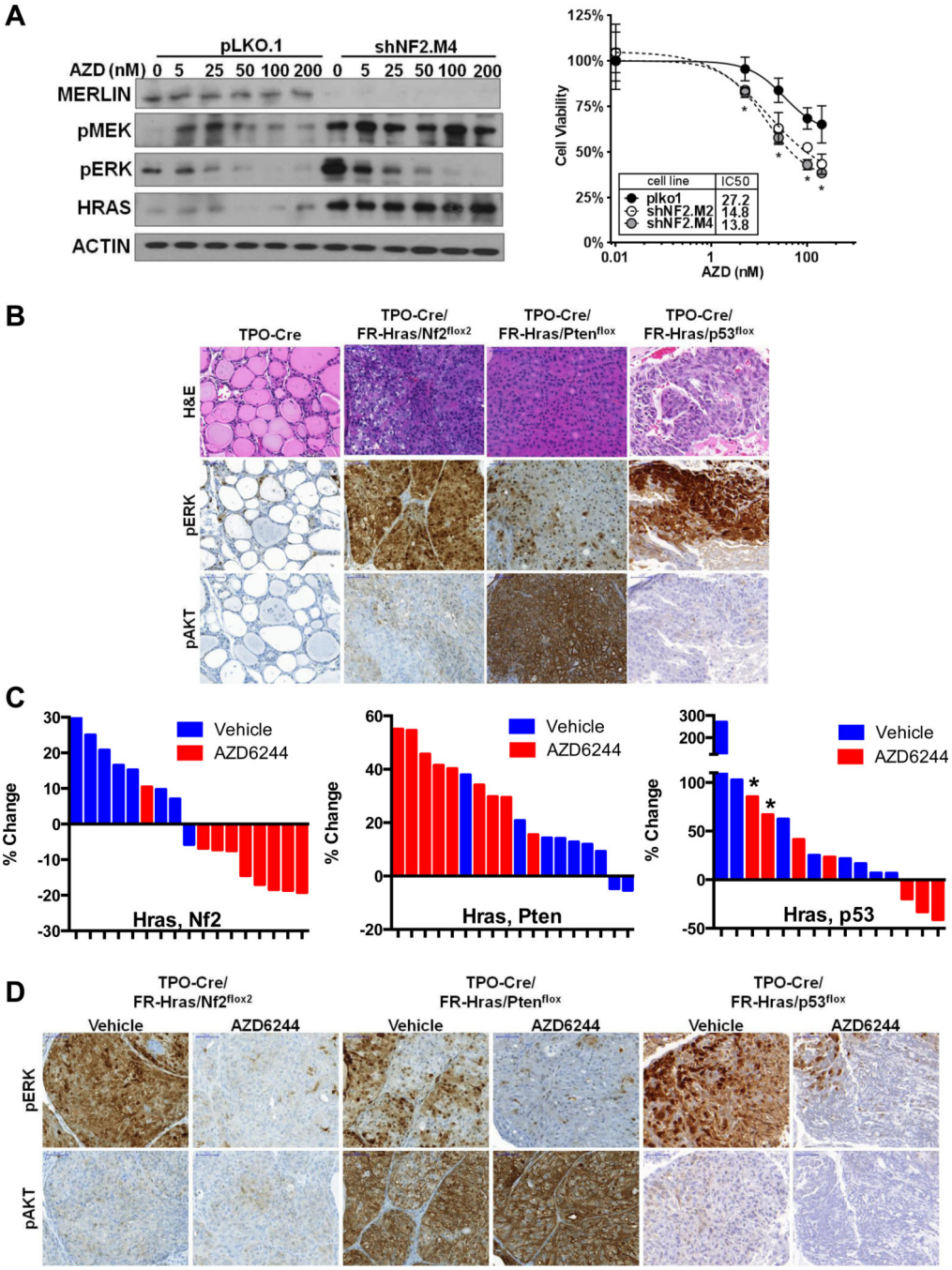

Figure 6. Merlin deficient RAS mutant cells and murine PDTCs are more sensitive to MEK inhibition

A) *Left:* Western blots of C643 cells expressing scrambled or shNF2.M4 for pMEK, pERK and HRAS after incubation with AZD6244 for 1h. *Right:* Growth inhibitory effects of AZD6244 in C643 (*HRAS*^{G13R}*NF2-WT*) cells stably expressing scrambled or 2 different NF2 shRNAs (M2 and M4). Cells were counted at 6 days. (n=3). Average IC50 of two replicate experiments is shown. *p<2 × E-2.

Author Manuscript Author Manuscript Author Manuscript Author Manuscript

B) H&E, pERK and $pAKT_{S473}$ IHC of representative thyroid cancer sections of each genotype.

C) Effect of *in vivo* treatment of thyroid cancers in *TPO-Cre/FR-Hras^{G12V}/NF2^{flox2}TPO-Cre/FR-Hras^{G12V}/PTEN^{flox2}* and *TPO-Cre/FR-Hras^{G12V}/p53^{flox2}* mice for 4 weeks with 25 mg/kg/b.i.d. AZD6244. Tumor volume was determined pre and post-treatment by ultrasound. Bars represent the percent change in tumor volume from baseline in each mouse. AZD6244 reduced tumor size in *Hras^{G12V}/NF2^{flox2}* mice (AZD6244 vs vehicle p= 3 × E-4); in *Hras^{G12V}/Pten^{flox2}* there was a paradoxical increase in tumor volume with the MEK inhibitor (p = 8 × E-4). AZD6244 had no significant effects on PDTC/ATC of *Hras^{G12V}/p53^{flox2}* mice (p=0.45). n=18 per group, Mann-Whitney test. *denotes ATC.

D) H&E, pERK and $pAKT_{S473}$ IHC of representative thyroid cancer sections of each genotype H&E-stained, pERK and $pAKT_{S473}$ IHC thyroid cancer sections in *TPO-Cre/FR-Hras^{G12V}/NF2^{flox2}TPO-Cre/FR-Hras^{G12V}/PTEN^{flox2}* and *TPO-Cre/FR-Hras^{G12V}/p53^{flox2}* mice treated with AZD6244 or vehicle.

Author Manuscript Author Manuscript Author Manuscript Author Manuscript

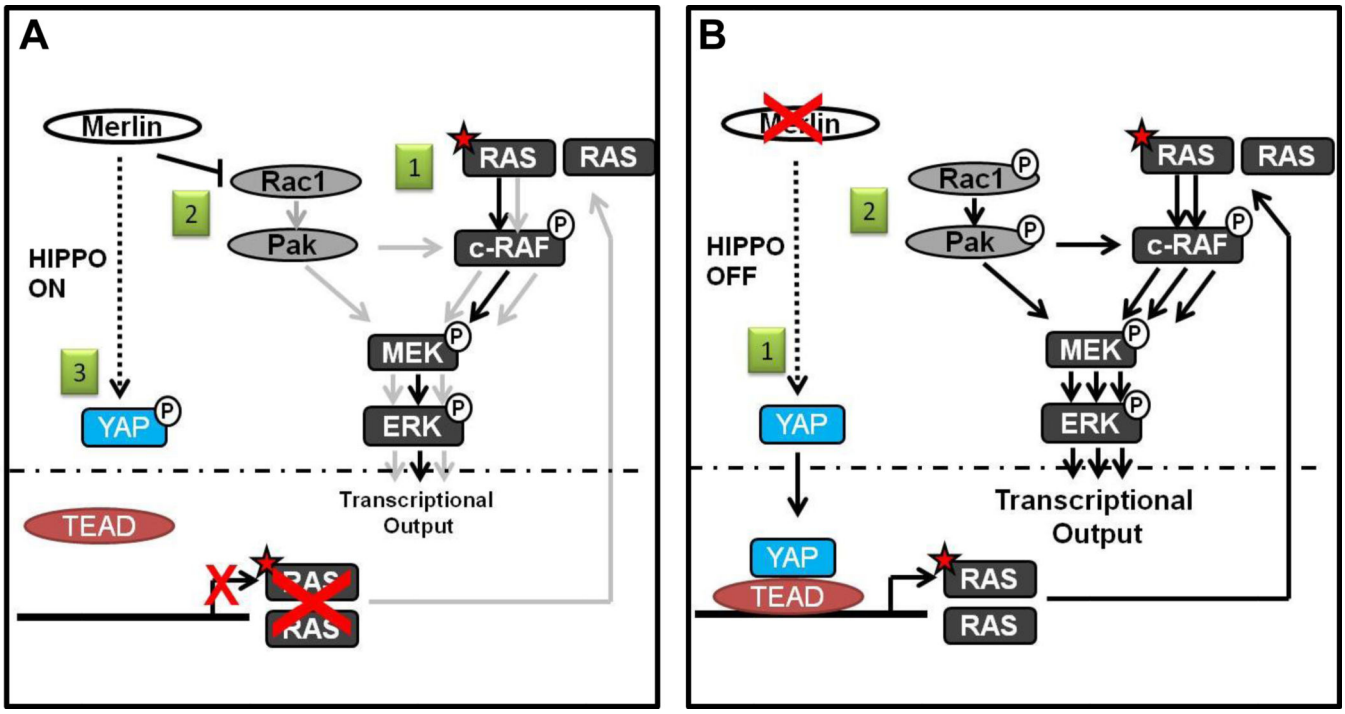

Figure 7. Mechanisms by which merlin loss cooperates with oncogenic RAS to induce thyroid tumorigenesis

A) In the presence of wild-type merlin, mutant *RAS* modestly increases MAPK signaling, which is insufficient to drive tumorigenesis (1). Wild-type merlin blocks RAC1 activation, decreasing stimulatory input of PAK into CRAF and pMEK (2). Merlin also activates the Hippo pathway, leading to phosphorylation of YAP and its retention in the cytoplasm. In the absence of nuclear YAP, TEAD is unable to induce transcription of wild-type and oncogenic RAS, restricting the magnitude of the oncogenic drive (3).

B) In Merlin-deficient cells the Hippo pathway is off (1), allowing YAP to form transcriptionally active complexes with TEAD, leading to increased oncogenic and wild-type RAS gene expression. This, in concert with engagement of RAC1-PAK signaling (2), leads to increased of MAPK output and promotion of tumorigenesis, while generating increased dependence on the pathway for viability.